Journal of Magnetics 27(4), 347-355 (2022)

ISSN (Print) 1226-1750
ISSN (Online) 2233-6656
https://doi.org/10.4283/JMAG.2022.27.4.347

# Significance of Chemical Processes and Non-uniform Heat Sink/source Aspects for Time-dependent Polymer Liquid Carrying Nanoparticles

**Zubair Hussain[1], Mehboob Ali[1]*, and Waqar Azeem Khan[1,2]**

[1]*Department of Mathematics, Mohi-ud-Din Islamic University, Nerian Sharif, Azad Jammu and Kashmir 12010, Pakistan*
[2]*Nonlinear Analysis and Applied Mathematics (NAAM) Research Group, Department of Mathematics, Faculty of Science, King Abdulaziz University, P. O. Box 80207, Jeddah 21589, Saudi Arabia*

(Received 18 August 2021, Received in final form 1 October 2022, Accepted 6 October 2022)

**Owing to extensive application developments of nanofluid, the engineers and scientists have concentrated their attention in regions of thermal and engineering processes. Additionally, nanofluids have wide-ranging returns as compared to traditional fluids. Keeping aforementioned logicality of nanofluid in observation, we deliberated a time-varying mathematical model to formulate the non-uniform heat sink-source assume Sutterby liquid over Brownian movements and thermophoretic. Thermal- solutal stratification phenomenon in addition with heat sink-source and activation energy aspects are scrutinized. Characteristics of random motion and thermophoresis diffusion properties for Sutterby fluid are examined. Similarity variable techniques are used to reduce partial differential equations into ordinary differential equations and solved numerically by using bvp4c method. The physical aspects of fluid flow, temperature, concentration for variation of involved parameters have been explained through graphs. Velocity of Sutterby nanofluid has contrary performances against unsteady and mixed convection parameters. Augmented values of Brownian moment, thermophoresis and heat source parameters exaggerate the temperature of nanofluid. Concentration of Sutterby nanofluid deteriorates for greater Schmidt number. Moreover, transportation rate of heat dwindles against Pr while it rises against $N_t$.**

**Keywords :** MHD nanofluid, sutterby fluid, thermal stratification, solutal stratification, heat generation/absorption

## 1. Introduction

Energy is the most significant and a special issue of any country from economic point-of-view because it is a plays key role for almost all other consumption as well as production processes. Therefore, energy is an essential factor that controls growth and determines many aspects of human activity. Energy [1-3] is not only consume in the industry but we also consume a lot of energy for the domestic necessities of mankind. Conventionally, fossils fuels are the energy sources which fulfil all these demands but it causes climate changes and environmental pollution. The extraction process which convert crude oil among practical fuels requires enormous energy, financial expenditures along with effort. Moreover, further utilization of fusels for various purposes produces several harmful compounds which have harmful effects for atmosphere and ultimately lead to pollution. Removal of pollution from the atmosphere again involves huge costs. Therefore, the use of these resources has become a major concern and researchers are working on alternatives. Therefore, (SEG) sustainable energy generation plays a significant role that can handle the existing situation. Not only these conventional energy sources cause global warming and pollution but there is a severe thread for the demand of future energy because of their diminution. This imposes itself on the development of new technologies which are established through renewable energy sources. Therefore, now a day's concentration is given to energy causes like wind energy, solar and geothermal energy. Heat energy that is used over transportation processes can be extracted from global, natural and abundant (sun) resources available. Moreover, development of technologies makes it to convert solar radiation into (EE) electrical energy. Through solar energy, we can reduce carbon dioxide emissions for reduction of global warming. The biggest challenge is how to effectively use and maximize these resources to meet most energy needs. Utilization of (SE) solar energy can usually be achieved through the (SPS) solar photovoltaic


*Corresponding author: Tel: +923471213394
Fax: +92-997-531551, e-mail: mehboob_maths@hu.edu.pk

structure, (STS) solar thermal structure and their arrangement. SPS use photovoltaic (PV) cells which convert SE into electrical energy. Through solar collectors, solar energy is converted into heat which is effectively used for cooling/heating purposes. The technology of solar liquid heating system utilizing solar radiation is efficient choice. The rapid advancements of thermal engineering and industrial procedures nowadays involve more and more condensed and proficient heat transfer classifications. Heat transfer is a communal phenomenon in environment due to the temperature alteration among substances or within a sole entity. The procedure of heat transfer phenomenon is of excessive attention and has received prodigious consideration from engineers and researchers owing to its extensive application in manufacturing development and engineering usage. Discovery of the right functioning fluid is the foremost assignment of researchers and is of inordinate importance.

Nano-science is helping them by delivering innovative functioning fluids. In mentioned heat transfer structures, a liquid is used as the coolant. Yet, these liquids have truncated thermal conductivity that could strictly distress the speed of heat transfer or cooling procedures. Enlightening the thermal conductivity of liquids is a stimulating assignment for researchers and scientists. Radiation possessions have extensive applications in the field of physics, manufacturing and industrial yields, like production of polymer dispensation, glass, nuclear apparatuses and aerospace technology. Sunlight, likewise entitled cosmological radiation, is a practice of radiation accomplished from the sun.

Magnetic fluid is widely applied as an innovative operational fluid. It is prepared of magnetic nanoparticles uniformly distributed and suspended in the base fluid, which could be adjusted by an external magnetic field. The outcomes of thermal radiation on the speed and temperature transfer process is due to its effects in fluidized bed heat exchangers, turbid water bodies, photochemical reactors, nuclear power plants, aircraft, missiles, satellites and spacecraft. Some other developments on nanofluids have been described in Refs. [4-33].

Recently, flows of non-Newtonian fluids [34-42] have fascinated the focus of several researchers. Due to the variety of non-Newtonian fluids in everyday life, their flow cannot be determined solely by the stress-strain relationship. Oil and grease, paper products, drilling muds, clay coating and suspensions, hot rolling are some illustrations of non-Newtonian fluids. The resulting equations are of advanced order and supplementary complex as associated to the Navier-Stokes equations. Therefore, it is challenging to construct an exact solution for the dependence equations in non-Newtonian fluids.

The reason for the non-linear relationship between shear stress and strain rate resulting from these non-Newtonian fluids is extensively applied in innumerable fields such as biology, technology, food processing and industry. Numerous rheological models have been proposed to analyze non-Newtonian fluids, but one model cannot designate all possessions of the fluid. One of the utmost communal models for relating non-Newtonian fluids is the Satterby fluid model that illuminates the possessions of aqueous solutions of polymer. Hayat *et al.* [43] explicated peristaltic properties obey the Darcy relationship when using Sutterby fluid. The numerical investigation of sutterby fluid with nanoparticles is implemented by Khan *et al.* [44]. The features of of Sutterby liquid employing nonlinear phenomenon of radiation is investigated by Khan *et al.* [45]. The aspects of melting sensation with Sutterbye liquid is clarified by Waqas *et al.* [46].

Considering into interpretation all the aforementioned applications, the purpose of current investigation is to examine the phenomenon of solutal and thermal stratification for Sutterby fluid. The novelty of the existing explored work is based unambiguously on five dimensions. Initially, we studied the time-dependent circumstance of the Sutterby liquid. Secondly, to analyze features of Brownian motion and thermophoretic. Thirdly to detect the phenomenon of non-uniform heat sink source. Fourthly, to conduct exploration in the occurrence of of thermal-solutal stratification phenomenon. Fifthly to buil solutions of the nonlinear phenomenon. Furthermore, influence of heat sink/source explored here in energy equation. Features of random motion of nanoparticles and also the influence of temperature variance on the nanoparticle is measured in this exertion. Suitable similarity transfiguration are employed to transmute the prevailing PDEs into ODEs. The procedure bvp4c in MATLAB is utilized to estimate numerical solutions for the velocity, temperature, and concentration equations. The accomplished consequences are demonstrated graphically and inspected comprehensively.

## 2. Technical Depiction and Flow Field Equations

Here, we have considered thermal-solutal stratification phenomenon for time-dependent 2D flow of Sutterby nanofluid. Here motion of Sutterby nanofluid occur because of stretching surface with velocity $\left[U_w = \frac{bx}{1-at}\right]$. The relation for energy equation is modeled via heat absorption-generation. Additionally, we have incorporated the Buongiorno model over random diffusion and thermophoresis associations for Sutterby nanofluid. We considered the wall and ambient temperature and concentration to be $T_w > T_\infty$, $C_w > C_\infty$. The problem discussed overhead governs the following system of equations:

$$\frac{\partial u}{\partial x}+\frac{\partial v}{\partial y}=0, \quad (1)$$

$$\frac{\partial u}{\partial t}+u\frac{\partial u}{\partial x}+v\frac{\partial u}{\partial y}=\upsilon\frac{\partial^2 u}{\partial y^2}\left[1-\frac{\beta^2}{6}\frac{\partial u}{\partial y}\right]^n-\frac{n\upsilon\beta^2}{6}\frac{\partial u}{\partial y}\frac{\partial^2 u}{\partial y^2}\left[1-\frac{\beta^2}{6}\frac{\partial u}{\partial y}\right]^{n-1} -\frac{\sigma B_0^2}{\rho}u+g\left[(1-C_\infty)\beta_T(T-T_\infty)-\frac{(\rho^*-\rho)}{\rho}(C-C_\infty)\right], \quad (2)$$

$$\frac{\partial T}{\partial t}+u\frac{\partial T}{\partial x}+v\frac{\partial T}{\partial y}=\frac{\kappa}{c_p\rho}\frac{\partial^2 T}{\partial y^2}+\tau^*\left[(\frac{\partial C}{\partial y}\frac{\partial T}{\partial y})D_B+(\frac{\partial T}{\partial y}\frac{\partial T}{\partial y})\frac{D_T}{T_\infty}\right]+\frac{1}{\rho c_p}q''', \quad (3)$$

$$\frac{\partial C}{\partial t}+u\frac{\partial C}{\partial x}+v\frac{\partial C}{\partial y}=\frac{D_T}{T_\infty}\frac{\partial^2 T}{\partial y^2}+D_B\frac{\partial}{\partial y}(\frac{\partial C}{\partial y})-k_r^2\left(\frac{T}{T_\infty}\right)^p(C-C_\infty)\exp\left(-\frac{E_a}{KT}\right), \quad (4)$$

with

$$q'''=\frac{k_n f^a}{\upsilon_f}\left[A^*(T_w-T_\infty)f'+B^*(T-T_\infty)\right], \quad (5)$$

$$u=U_w=\frac{bx}{1-at},\ v=0, T=T_w=T_0+\frac{Ax}{1-at},\ C=C_w=C_0+\frac{Dx}{1-at}, \text{at } y=0 \quad (6)$$

$$u\to 0,\ T\to T_\infty=T_0+\frac{Bx}{1-at},\ C\to C_\infty=C_0+\frac{Ex}{1-at}\ \text{ as } y\to\infty. \quad (7)$$

We utilize the transformations:

$$\eta=y\sqrt{\frac{b}{v(1-at)}},\ u=\frac{bx}{1-at}f'(\eta),\ v=-\sqrt{\frac{bv}{1-at}}f(\eta), \theta(\eta)=\frac{T-T_\infty}{T_w-T_0},\ \varphi(\eta)=\frac{C-C_\infty}{C_w-C_0}. \quad (8)$$

Here $f'(\eta)$, $\theta(\eta)$ and $\phi(\eta)$ depicts the non-dimensionalized velocity, temperature and concentration. Eq. (1) is fulfilled identically. Moreover, utilizing expression (7) into the expressions (2)-(6), we get the differential systems as follows:

$$\left[1-\frac{\alpha}{6}f''\right]^n f'''-\frac{n\alpha}{6}\left[1-\frac{\alpha}{6}f''\right]^{n-1}f''f'''-f'^2+ff''-\tau(f'+\frac{1}{2}\eta f'') -Mf'+R_a[\theta+N_r\phi]=0, \quad (9)$$

$$\theta''+\Pr\left[f\theta'+N_b\theta'\phi'+N_t\theta'^2-S_tf'-f'\theta-\tau S_t\right] +\Pr\left[-\tau\frac{\eta}{2}\theta'-\tau\theta\right]+(A_1f'+B_1\theta)=0, \quad (10)$$

$$\phi''+\frac{N_t}{N_b}\theta''-Sc\left[(1+\delta\theta)^p\phi\exp\left(-\frac{E}{1+\delta\theta}\right)\right] -Sc\left[\tau\phi+\eta\tau\phi'+\tau S_m+f'\phi+S_mf'-f\phi'\right]=0, \quad (11)$$

$$f(0)=0,\ f'(0)=1, \theta(0)=1-S_t,\ \phi(0)=1-S_m, \quad (12)$$

$$\theta(\infty)\to 0,\ \phi(\infty)\to 0,\ f'(\infty)\to 0, \quad (13)$$

where

$$M=\frac{\sigma B_0^2(1-at)}{\rho b}, N_r=\frac{(\rho^*-\rho)}{\rho}\frac{(C_w-C_0)}{(1-C_\infty)\beta_T(T_w-T_0)}, \tau=\frac{a}{b}, \Pr=\frac{C_p\rho\nu}{\kappa},$$
$$R_a=\frac{g\left[(1-C_\infty)\beta_T(T_w-T_0)(1-at)^2\right]}{b^2x}, N_b=\frac{\tau D_B(C_w-C_0)}{\upsilon}, N_t=\frac{\tau D_T(T_w-T_0)}{\nu T_\infty},$$
$$S_m=\frac{E}{D}, S_t=\frac{B}{A}, S_c=\frac{\nu}{D_B}, E=\frac{E_a}{\kappa T_\infty}, \delta=\frac{T_w-T_0}{T_\infty},$$
$$\alpha=\frac{\beta^2 bx\sqrt{b}}{(1-at)^{\frac{3}{2}}\sqrt{\nu}}, A_1=\frac{(1-at)U_wA^*(A-B)}{Abx}, B_1=\frac{(1-at)U_wB^*A}{Abx}$$

### 2.1 Physial quantities

The expressions for the local Nusselt number (rate of heat transfer), local sherwood number (rate of mass transfer) and skin-friction coefficient are well-defined by

$$C_{fx}=\frac{\mu}{\rho U_w^2}\left[1-\frac{\beta^2}{6}\left(\frac{\partial u}{\partial y}\right)\right]^n\frac{\partial u}{\partial y}, \quad (14)$$

$$Nu_x=\frac{-x}{(T_w-T_\infty)}\frac{\partial T}{\partial y}, \quad (15)$$

$$Sh_x=\frac{-x}{(C_w-C_\infty)}\frac{\partial C}{\partial y}, \quad (16)$$

Dimensionless form of above quantities is given by

$$C_{fx}\mathrm{Re}_x^{1/2}=\left[1-\frac{\alpha}{6}f''(0)\right]^n f''(0), Nu_x\mathrm{Re}_x^{-1/2}=-\left[\frac{1}{1-S_t}\right]\theta'(0), Sh_x\mathrm{Re}_x^{-1/2}=-\left[\frac{1}{1-S_m}\right]\phi'(0), \quad (17)$$

where $\mathrm{Re}_x=\frac{xU_w}{\nu}$ signifies local Reynolds number.

## 3. Solution Methodologies

### 3.1. MATLAB tool bvp4c technique

The present component, we have recommended a numerical solution of overhead declared ODEs (9-11) with conditions (12, 13). The procedure is specified as follows:

$$f=Q_1,\ f'=Q_2,\ f''=Q_3,\ f'''=Q_3', \quad (18)$$

$$\theta=Q_4,\ \theta'=Q_5,\ \theta''=Q_5', \quad (19)$$

$$\phi=Q_6,\ \phi'=Q_7\ \ \phi''=Q_7', \quad (20)$$

where

$$Q_3'=\frac{Q_2^2-Q_1Q_3+\tau(Q_2+\frac{1}{2}\eta Q_3)-MQ_2+R_a(Q_4+N_rQ_6)}{A_1}, \quad (21)$$

$$Q_5' = -\Pr\left[Q_1Q_5 + N_bQ_5Q_7 + N_tQ_5^2 - S_tQ_2 - Q_2Q_4\right] - \Pr\left[-\tau S_t - \tau\frac{\eta}{2}Q_5 - \tau Q_4\right] - \left(A_1Q_2 + B_1Q_4\right), \quad (22)$$

$$Q_7' = -\frac{N_t}{N_b}Q_5' + Sc\left[\left(1+\delta Q_4\right)^p Q_6 \exp\left(-\frac{E}{1+\delta Q_4}\right) + \tau Q_6 + \eta\tau Q_7\right] + Sc\left[\tau S_m + Q_2Q_6 + S_mQ_2 - Q_1Q_7\right], \quad (23)$$

here

$$A_1 = \left[1-\frac{\alpha}{6}Q_3\right]^n - \frac{n\alpha}{6}\left[1-\frac{\alpha}{6}Q_3\right]^{n-1}Q_3, \quad (24)$$

with

$$Q_1(0)=0,\ \ Q_2(0)=1,\ \ Q_4(0)=1-S_t,\ Q_6(0)=1-S_m, \quad (25)$$

$$Q_2 \to 1\ \ Q_4 \to 0,\ Q_6 \to 0\ \text{ as }\ \eta \to \infty. \quad (26)$$

## 4. Results and Discussion

The main theme of this division is to interpret the physical behavior of Sutterby nanofluid against numerous pertinent parameters. Significant aspects of evolving variables like Unsteady parameter ($\tau$), magnetic parameter ($M$), Schmidt number ($Sc$), mixed convection parameter ($Ra$), Brownian motion parameter ($N_b$), Sink parameter ($B_1$), thermophoresis parameter ($N_t$), Prandtl parameter (Pr) and chemical reaction parameter ($L$) on velocity $f(\eta)$, temperature $\theta(\eta)$ and concentration $\phi(\eta)$ are inspected via graphs in this part. This goal is accomplished through plan of Figs. 1-12. Fig. 1. represents the impact of $M$ on $f'$. Here $f'$ decays via larger $M$. Physically, rise in the Lorentz force bases a proportion of conflict for Sutterby nanofluid that dwindles the liquid velocity. In definite physical circumstances, it has been designated that the magnetic fiels diminishes the velocity of fluid elements or we observed that that the drag force relates normally to the stretched plane and consequently diminishes the Sutterby fluid drive. The magnetic parameter is linked to the Lorentz force that occurs as of the magnetic and electrical forces simultaneously. Characteristics of $f'$ for fluctuating $Ra$ are designated in Fig. 2. Mixed convection parameter $Ra$ has a direct relation with fluid velocity $f'$, due to buoyancy force. Fig. 3 establish the relation between $f'$ and $\tau$. Here $f'$ decays when $\tau$ is incremented. Increasing the unsteady parameter decreases velocity profile.

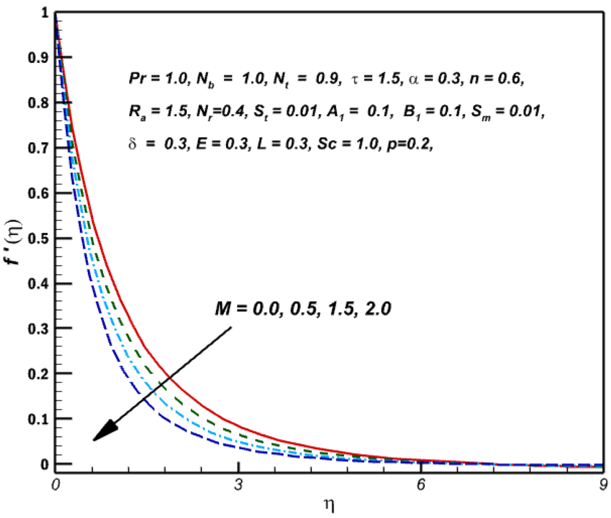


**Fig. 1.** (Color online) $f'(\eta)$ impact for different $M$.

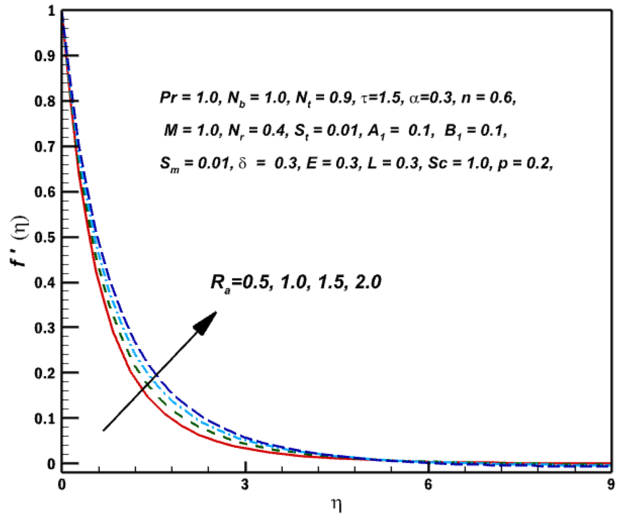


**Fig. 2.** (Color online) $f'(\eta)$ impact for different $R_a$.

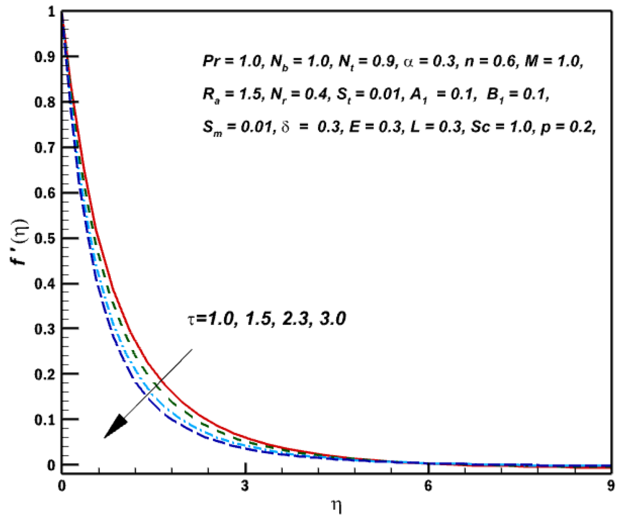


**Fig. 3.** (Color online) $f'(\eta)$ impact for different $\tau$.

Fig. 4 portrays the impact of $B_1$ against $\theta$. It is observed that $\theta$ rises for larger. Physically, heat is added to fluid for larger $B_1$ due to which temperature of nanofluid rises. Fig.

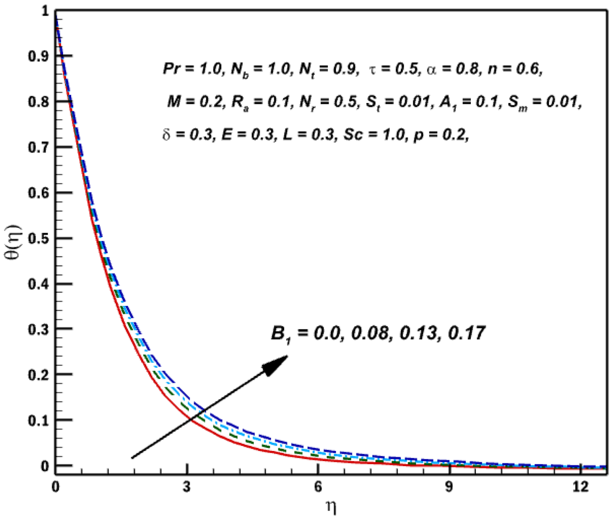


**Fig. 4.** (Color online) $\theta(\eta)$ impact for different $B_1$.

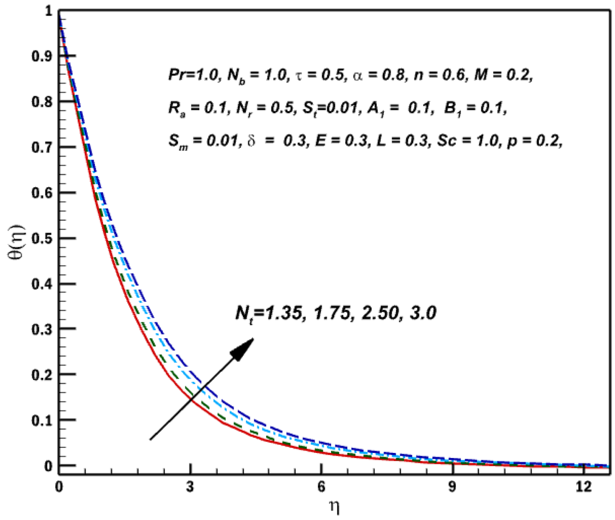


**Fig. 6.** (Color online) $\theta(\eta)$ impact for different $N_t$.

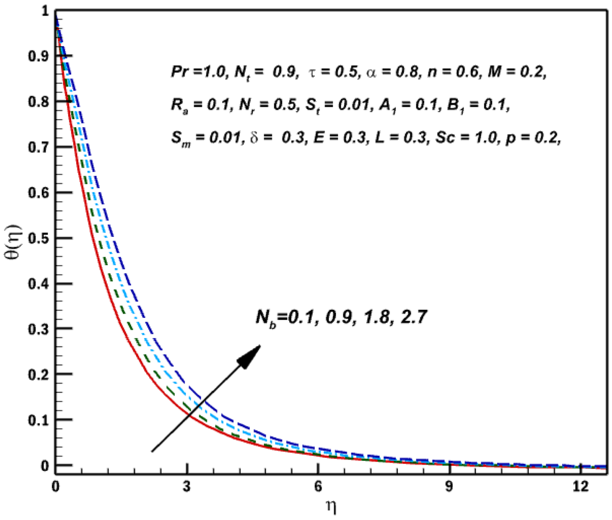


**Fig. 5.** (Color online) $\theta(\eta)$ impact for different $N_b$.

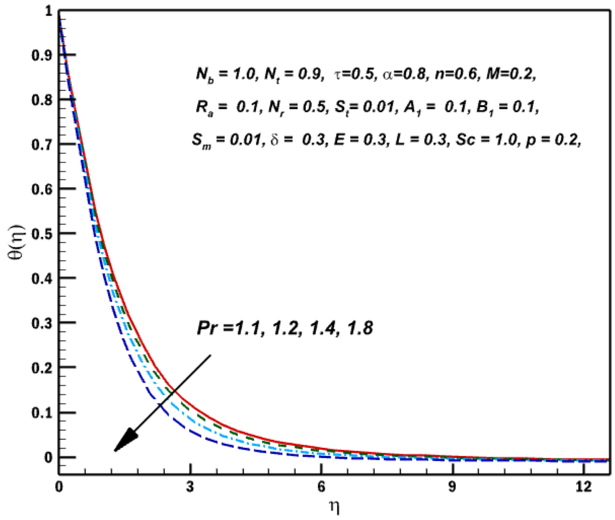


**Fig. 7.** (Color online) $\theta(\eta)$ impact for different Pr.

5 is kecked to portray the impact of $N_b$ against $\theta$. For larger $N_b$ diminishing behavior of $\theta$ is seen. These graphs illustrates dominant behavior of $\theta(\eta)$ when rises $N_b$. In fact $D_B$ (Brownian moment coefficient) rises for lager $N_b$. As a consequence of particle collusion, temperature of the collided particle enhances, and they become less dense simultaneously. On top of that (due to convection phenomenon) less dense particles transfer from the section of sophisticated temperature to the lower temperature. Because of that, the overall temperature of the liquid rises. Consequently, $\theta(\eta)$ rises. Consequence of $N_t$ (thermophoresis diffusion) for $\theta(\eta)$ is highlighted in Fig. 6. Clearly, $\theta(\eta)$ boosts for larger $N_t$. In fact gradient of temperature rises for intensified vales of $N_t$. Moreover, we have observed that in case of $N_t$ heat transfer process mainly depend on convection which essentially occur due to temperature gradien. So, $\theta(\eta)$ rises for grater $N_t$. Fig. 7 stipulates the possessions of Pr (Prandtl number) for $\theta(\eta)$. From Fig. we clearly demonstrate the declining manners of $\theta(\eta)$ for superior Pr. In fact, the thermal diffusivity of nanofluid declines by enhancing Pr. So, $\theta(\eta)$ decreases. Variation for $\theta(\eta)$ (temperature) of liquid via $\tau$ (time-dependent parameter) is captured in Fig. 8. Graphical behavior shows that $\theta(\eta)$ dwindles for larger $\tau$.

The stimulating performance of $N_b$ (Brownian moment parameter) for $\theta(\eta)$ is delivered in Fig. 9. Diminishing conduct of $\theta(\eta)$ is perceived for $N_b$. Fig. 10 postulates the possessions of $N_t$ (thermophoresis parameter) for $\theta(\eta)$. This Fig. evidently clarifies the intensifying conduct of $\theta(\eta)$ for better $N_t$. Substantially, thermophoretic forces

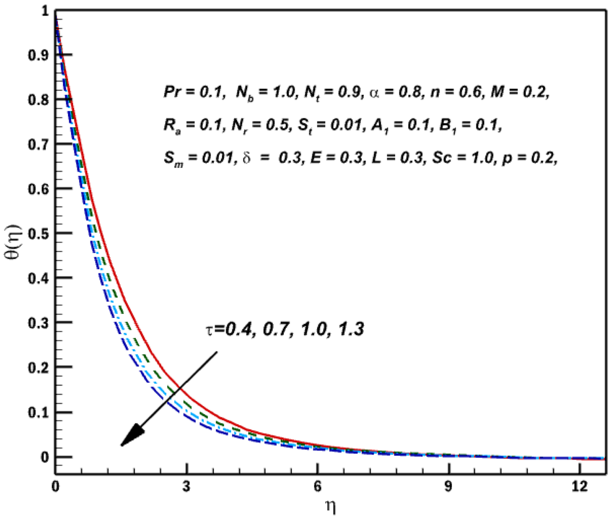


**Fig. 8.** (Color online) $\theta(\eta)$ impact for different Pr.

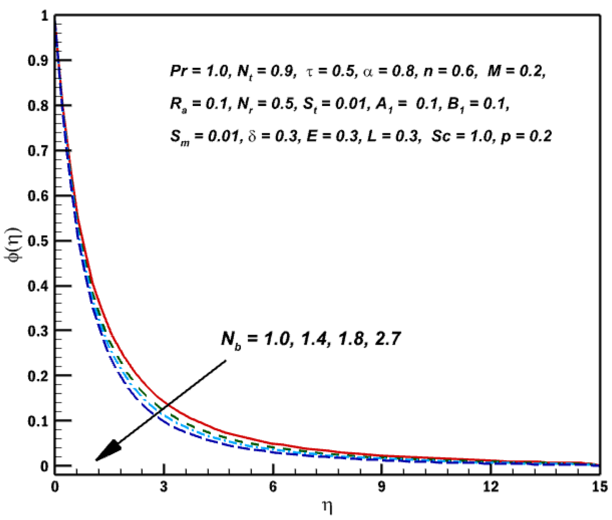


**Fig. 9.** (Color online) $\phi(\eta)$ impact for different $N_b$.

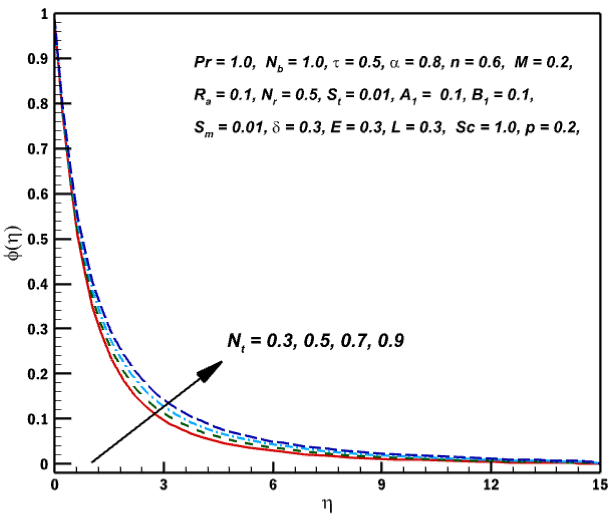


**Fig. 10.** (Color online) $\phi(\eta)$ impact for different $N_t$.

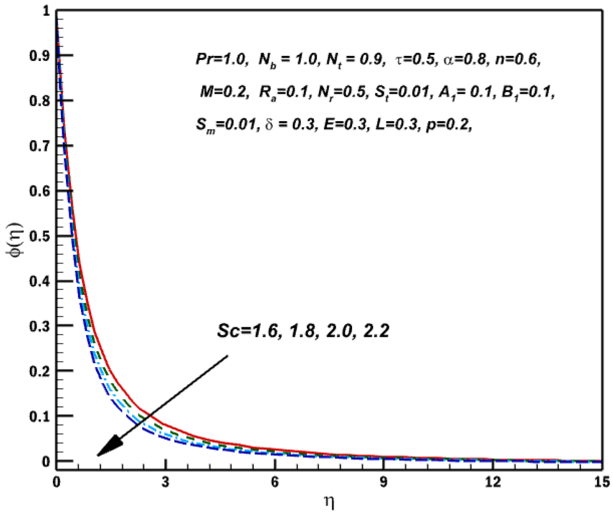


**Fig. 11.** (Color online) $\phi(\eta)$ impact for different *Sc*.

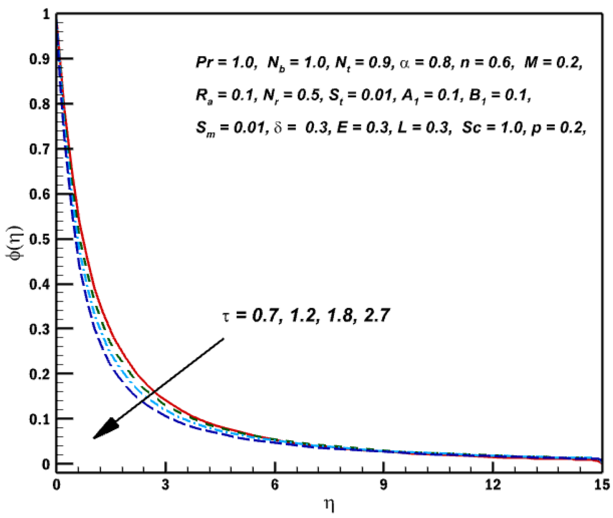


**Fig. 12.** (Color online) $\phi(\eta)$ impact for different $\tau$.

rises for outstanding $N_t$. So, $\theta(\eta)$ exaggerates for more $N_t$.

The significance role of *Sc* (Schmidt number) on of liquid is specified over Fig. 11. It is found that concentration $\phi(\eta)$ of Sutterby fluid is deteriorating role of *Sc*. Actually, *Sc* depends on $D_B$ (Brownian moment coefficient) besides for enhanced *Sc*, $\phi(\eta)$ inclines to dwindles (Brownian moment coefficient) that reveals the feebler nanoparticle concentration profile. Fig. 12. highlights the features of $\tau$ for $\phi(\eta)$. These graphs demonstrates prominent behavior of $\tau$ on $\phi(\eta)$. This Fig. shows the diminishing behavior $\phi(\eta)$ for larger $\tau$.

### 4.1. Characteristics of surface drag force and heat-mass transfer rate

To authenticate the present data, Table 1 displays the association of $Nu_x \mathrm{Re}_x^{-1/2}$ using the available assignment

**Table 1.** Comparison of $Nu_x \mathrm{Re}_x^{-1/2}$ when $\tau = R_a = \alpha = S_t$, $A_1 = B_1 = 0$.

| $Nu_x \mathrm{Re}_x^{-1/2}$ | | | |
|---|---|---|---|
| $N_b$ | $N_t$ | Saif-ur-Rehman *et. al.* [47] | Present |
| 0.1 | 0.1 | 0.29570 | 0.29570 |
| 0.2 | - | 0.28845 | 0.28845 |
| 0.3 | - | 0.28125 | 0.28125 |
| 0.1 | 0.1 | 0.29570 | 0.29570 |
| 0.1 | 0.2 | 0.28984 | 0.28984 |
| 0.1 | 0.3 | 0.27419 | 0.27419 |

**Table 2.** Surface drag force $C_{fx} \mathrm{Re}_x^{1/2}$ through diverse estimation of $M$, $R_a$, $\tau$ and $\alpha$ when $A_1 = B_1 = 0.1$, $E = L = \delta = 0.3$, $I_r = 0.4$, $S_m = S_t = 0.01$, $S_c = \mathrm{Pr} = 0.7$, $N_b = 0.1$, $N_t = 0.9$, $\alpha = 0.3$, $n = 0.9$, $p = 0.2$.

| $C_{fx} \mathrm{Re}_x^{1/2}$ | | | | | |
|---|---|---|---|---|---|
| $M$ | $R_a$ | $\tau$ | $\alpha$ | bvp4c technique | GDQM |
| 0.1 | 0.3 | 0.4 | 0.3 | -1.096363 | -1.096363 |
| 0.5 | - | - | - | -1.26246 | -1.26246 |
| 0.9 | - | - | - | -1.411266 | -1.411266 |
| 1.3 | 0.5 | - | - | -1.553036 | -1.553036 |
| - | 0.7 | - | - | -1.491935 | -1.491935 |
| - | 0.9 | - | - | -1.432335 | -1.432335 |
| - | - | 0.6 | - | -1.499100 | -1.499100 |
| - | - | 0.8 | - | -1.562170 | -1.562170 |
| - | - | 1.0 | - | -1.622276 | -1.622276 |
| - | - | - | 0.6 | -1.716743 | -1.716743 |
| - | - | - | 0.9 | -1.810140 | -1.810140 |
| - | - | - | 1.2 | -1.902701 | -1.902701 |

of Saif-ur-Rehman *et al.* [47]. We detected through Table 1 where our consequences gives exceptional settlement with published exertion. Table 2 shows the comparison between GDQM (generalized differential quadrature method) and bvp4c technique in MATLAB. Tabular form shows excellent agreement between these two techniques. Table 2 shows that surface drag force declines for higher $M$, $\tau$, $\alpha$ and growths via longer $R_a$. Table 3 represents the features of $N_b$, $N_t$, $\tau$, $c$ and $Sc$ on heat-mass transmission rate. It is perceived that local Nusselt number exaggerates through bigger $\tau$, Pr and it decreases for greater $N_b$, $N_t$ and $S_c$. Whereas, local sherwood number rises for more $N_b$, $\tau$, $S_c$ and deteriorates for greater $N_t$ and Pr.

**Table 3.** Local Nusselt number $\mathrm{Re}^{-1/2} Nu_x$ and local sherwood number $Sh_x \mathrm{Re}_x^{-1/2}$ via different estimation of $N_b$, $N_t$, $\tau$, Pr and $Sc$ when $A_1 = B_1 = 0.1$, $E = L = \delta = 0.3$, $N_r = 0.5$, $S_m = S_t = 0.01$, $\mathrm{Pr} = 1.0$, $\alpha = 0.8$, $M = 0.2$, $n = 0.6$, $p = 0.2$, $R_a = 0.1$.

| $N_b$ | $N_t$ | $\tau$ | Pr | $Sc$ | $\mathrm{Re}^{-1/2} Nu_x$ | $Sh_x \mathrm{Re}_x^{-1/2}$ |
|---|---|---|---|---|---|---|
| 0.1 | 0.2 | 0.3 | 1.0 | 1.0 | 0.897464 | 0.848443 |
| 0.3 | - | - | - | - | 0.837380 | 1.06845 |
| 0.5 | - | - | - | - | 0.779965 | 1.11384 |
| 0.7 | 0.3 | - | - | - | 0.711047 | 1.10935 |
| - | 0.4 | - | - | - | 0.696448 | 1.08507 |
| - | 0.5 | - | - | - | 0.68266 | 1.06082 |
| - | - | 0.4 | - | - | 0.716258 | 1.08998 |
| - | - | 0.5 | - | - | 0.748074 | 1.11924 |
| - | - | 0.6 | - | - | 0.778359 | 1.1482 |
| - | - | - | 1.1 | - | 0.808492 | 1.14806 |
| - | - | - | 1.3 | - | 0.858806 | 1.14782 |
| - | - | - | 1.5 | - | 0.898950 | 1.14763 |
| - | - | - | - | 1.1 | 0.888582 | 1.22021 |
| - | - | - | - | 1.2 | 0.879050 | 1.28953 |
| - | - | - | - | 1.3 | 0.870237 | 1.35598 |

## 5. Conclusions

In this investigation production, we have scrutinized the impact of mixed convection and activation energy on Sutterby nanofluid with stratification phenomenon. Additionally, non-uniform heat sink-source is added in the relation of energy expression. Thermal- solutal stratification phenomenon is scrutinized. Moreover, characteristics of random motion and thermophoresis diffusion properties for Sutterby fluid are examined. ODEs are obtained by utilizing similarity variable techniques. System of ODEs is then solved by using bvp4c method. The key results are as follows:

- By enhancing the $M$ (Magnetic parameter) and $\tau$ (time-dependent) the velocity of Sutterby nanofluid deteriorates.
- Velocity of Sutterby nanofluid intesifies for greater $R_a$ mixed convention parameter) decreases velocity.
- Temperature of Sutterby nanofluid has rises for larger values of $B_1$ (heat source parameter) $N_b$ (Brownian motion parameter) and $N_t$ (Thermophoresis parameter)
- By rising Pr (Prandtl number) and $\tau$ (time-dependent parameter) $\theta(\eta)$ decreases.
- Concentration of nanofuid $\phi(\eta)$ has reversed trend against $N_t$ and $N_b$.
- Transportation rate of heat dwindles against Pr while it rises against $N_t$ and $N_b$.
- Mass transportation rate deteriorates $N_t$.

## Nomenclature

*a*, *b*, *d*, *e*: Constants
$B_0$ : Magnetic field strength
$C$ : Nanoparticle volume fraction
$D_T$ : Thermophoretic diffusion coefficient
$D_B$ : Brownian diffusion coefficient
$A^*, B^*$ : Heat sink/source parameters
$C_\infty, T_\infty$ : Ambient Concentration/temperature
T : Temperature of nanofluid
k : Thermal conductivity
$k^*$ : Mean absorption coefficient
$k_r$ : Chemical reaction parameter
$g$ : Gravitational acceleration
$c_p$ : Specific heat
$E_a$ : Activation energy
$u$, $v$ : Velocity components
$C_f$ : Skin-friction coefficient
$\tau^*$ : Ratio of effective heat capacities
$\beta$ : Sutterby fluid parameter
$q_w$ : Wall heat flux
$R_a$ : Mixed convention parameter
$S_t$ : Thermal Stratification parameter
$\eta$ : Similarity variable
$S_m$ : Mass stratification parameter
$n$ : Power law index
$Pr$ : Prandtl number
$N_b$ : Brownian motion parameter
$N_t$ : Thermophoresis parameter
$\tau$ : Unsteadiness parameter
$Sc$ : Schmidt number
$M$ : Magnetic parameter
$N_r$ : Buoyancy ratio parameter
$f'$ : Dimensionless velocity
$\tau_w$ : Surface shear stress
$\phi$ : Dimensionless concentration
$J_w$ : Mass flux
$\theta$ : Dimensionless temperature
$\alpha$ : Sutterby fluid parameter
$A_1$, $B_1$ : Heat sink/source parameters
$\delta$ : Chemical reaction parameter
$Nu_x$ : Nusselt number
$Sh_x$ : Sherwood number

## References


[1] V. Chaurasiya, D. Kumar, K. N. Rai, and J. Singh, Therm. Sci. Eng. Prog. **20**, 100664 (2020).
[2] V. Chaurasiya, K. N. Rai, and J. Singh, J. Therm. Anal. Calorim. (2021). doi.org/10.1007/s10973-021-10614-8.
[3] V. Chaurasiya, K. N. Rai, and J. Singh, Therm. Sci. Eng. Prog. **25**, 101002 (2021).
[4] S. U. S. Choi, ASME Int. J. Mech. Eng. **66**, 99 (1995).
[5] J. A. Eastman, S. U. S. Choi, S. Li, W. Yu, and L. J. Thompson, Appl. Phys. Lett. **78**, 718 (2001).
[6] J. Buongiorno, ASME Int. J. Mech. Eng. **128**, 240 (2006).
[7] M. Ali, F. Sultan, W. A. Khan, M. Shahzad, H. Arif, and M. Irfan, International Journal of Numerical Methods for Heat & Fluid Flow **31**, 3304 (2021). https://doi.org/10.1108/HFF-04-2019-0334
[8] F. Sultan, W. A. Khan, M. Shahzad, M. Ali, and Z. Hussain, J. Therm. Anal. Calorim. **140**, 1069 (2020). https://doi.org/10.1007/s10973-019-08957-4
[9] Z. Hussain, A. ur Rehman, A. J. Shaikh, Kai-Xin Hu, M. Ali, F. Sultan, M. Shahzad, and M. Altanji, Case Studies in Thermal Engineering **26**, 100998 (2021).
[10] M. Ali, F. Sultan, M. Shahzad, and W. A. Khan, Indian J. Phys. **95**, 315 (2021). https://doi.org/10.1007/s12648-020-01706-6
[11] M. Ali, M. Shahzad, F. Sultan, and W. A. Khan, Appl. Nanosci. **10**, 3259 (2020). https://doi.org/10.1007/s13204-020-01385-z
[12] Z. Hussain, S. Zuev, A. Kabobel, M. Ali, F. Sultan, and M. Shahzad, Appl. Nanosci. **10**, 5211 (2020). https://doi.org/10.1007/s13204-020-01361-7
[13] Z. Hussain, M. Ali, M. Shahzad, and F. Sultan, Pramana - J. Phys. **94**, 49 (2020). https://doi.org/10.1007/s12043-019-1900-6
[14] W. A. Khan, M. Khan, and R. Malik, PLoS ONE **9**, e105107 (2014).
[15] W. A. Khan, H. Sun, M. Shahzad, M. Ali, F. Sultan, and M. Irfan, Indian J. Phys. **95**, 89 (2021). https://doi.org/10.1007/s12648-019-01678-2
[16] M. Shahzad, M. Ali, F. Sultan, W. A. Khan, and Z. Hussain, Indian J. Phys. **95**, 481 (2021). https://doi.org/10.1007/s12648-019-01669-3
[17] M. Khan and W. A. Khan, AIP Advances **6**, 025211 (2016). doi.org/10.1063/1.4942201.
[18] Z. Hussain, R. Zeesahan, M. Shahzad, M. Ali, F. Sultan, A. M. Anter, H. Zhang, and N. Khan, Pramana - J. Phys. **95**, 27 (2021). https://doi.org/10.1007/s12043-020-02043-3
[19] S. Z. Abbas, W. A. Khan, H. Sun, M. Ali, M. Waqas, M. Irfan, and S. Ahmad, J. Braz. Soc. Mech. Sci. Eng. **41**, 556 (2019). https://doi.org/10.1007/s40430-019-2050-y
[20] W. A. Khan, M. Irfan, M. Khan, A. S. Alshomrani, A. K. Alzahrani, and M. S. Alghamdi, J. Mol. Liq. **234**, 201 (2017).
[21] W. A. Khan, A. S. Alshomrani, A. K. Alzahrani, M. Khan, and M. Irfan, Pramana-J. Phys. **91**, (2018). doi.org/10.1007/s12043-018-1634-x.
[22] S. Khan, W. Shu, M. Ali, F. Sultan, and M. Shahzad, Appl. Nanosci. **10**, 5391 (2020). https://doi.org/10.1007/s13204-020-01546-0
[23] F. Sultan, S. Mustafa, W. A. Khan, M. Shahzad, M. Ali, W. Adnan, and S. Rehman, Appl. Nanosci. **10**, 3295 (2020). https://doi.org/10.1007/s13204-020-01294-1

[24] W. A. Khan, M. Waqas, M. Ali, F. Sultan, M. Shahzad, and M. Irfan, Int. J. Numer. Methods Heat Fluid Flow **29**, 3498 (2019).
[25] W. A. Khan, S. Farooq, S. Kadry, M. Hanif, F. J. Iftikhar, and S. Z. Abbas, Comput. Methods Programs Bio. **190**, 105355 (2020).
[26] W. A. Khan, M. Waqa, S. Kadry, Z. Asghar, S. Z. Abbas, and M. Irfan, Comput. Meth. Prog. Bio. **190**, 105347 (2020).
[27] F. Sultan, S. Mustafa, W. A. Khan, M. Shahzad, M. Ali, W. Adnan, and S. Rehman, Appl. Nanosci. **10**, 3295 (2020). https://doi.org/10.1007/s13204-020-01294-1
[28] W. A. Khan, M. Waqas, Wathek Chammam, Z. Asghar, U. A. Nisar, and S. Z. Abbas, Comput. Meth. Prog. Bio. **191**, 105396 (2020).
[29] W. A. Khan, M. Ali, M. Shahzad, F. Sultan, M. Irfan, and Z. Asghar, Appl. Nanosci. **10**, 3235 (2020). doi.org/10.1007/s13204-019-01220-0.
[30] Z. Hussain, A. U. Rehman, R. Zeeshan, F. Sultan, T. A. Hamid, M. Ali, and M. Shahzad, Appl. Nanosci. **10**, 5149 (2020). https://doi.org/10.1007/s13204-020-01308-y
[31] M. Ali, M. Shahzad, F. Sultan, W. A. Khan, and S. Z. H. Shah, Appl. Nanosci. **10**, 5201 (2020). https://doi.org/10.1007/s13204-020-01532-6
[32] W. A. Khan, M. Ijaz Khan, S. Kadry, S. Farooq, M. Imran Khan, and S. Z. Abbas, Neural. Comput. Applic. 32, 13565 (2020). doi.org/10.1007/s00521-020-04766-1.
[33] T. Hayat, Inayatullah, S. Momani, and K. Muhammad, Int. Commun. Heat Mass Transf. **126**, 105389 (2021).
[34] A. Hussanan, M. Z. Salleh, I. Khan, and S. Shafie, Journal of Molecular Liquids **229**, 482 (2017).
[35] S. Aman, I. Khan, Z. Ismail, M. Z. Salleh, and Q. M. Al-Mdallal, Sci. Rep. **7**, 2445 (2017). https://doi.org/10.1038/s41598-017-01358-3
[36] N. S. Khan, T. Gul, S. Islam, I. Khan, A. M. Alqahtani, and A. S. Alshomrani, Appl. Sci. **7**, 271 (2017). https://doi.org/10.3390/app7030271
[37] M. Sheikholeslami, Z. Shah, A. Shafee, I. Khan, and I. Tlili, Sci. Rep. **9**, 1196 (2019). https://doi.org/10.1038/s41598-018-37964-y
[38] G. Aaiza, I. Khan, and S. Shafie, Nanoscale Res. Lett. **10**, 490 (2015). https://doi.org/10.1186/s11671-015-1144-4
[39] A. Hussanan, Z. Ismail, I. Khan, A. G. Hussein, and S. Shafie, Eur. Phys. J. Plus **129**, 46 (2014). https://doi.org/10.1140/epjp/i2014-14046-x
[40] W. A. Khan and M. Ali, Appl. Phys. A **125**, 1 (2019).
[41] R. Ali, A. Shahzad, K. us Saher, Z. Elahi, and T. Abbas, Case Studies in Thermal Engineering **29**, 101695 (2022).
[42] T. Abbas, B. Ahmad, A. Majeed, T. Muhammad, and M. Ismail, Journal of Magnetics **26**, 277 (2021).
[43] T. Hayat, S. Ayub, A. Alsaedi, A. Tanveer, and B. Ahmad, Results Phys. **7**, 762 (2017).
[44] U. Khan, A. Shafiq, A. Zaib, A. Wakif, and D. Baleanu, Alex. Eng. J. **59**, 4851 (2020).
[45] W. A. Khan, N. Anjum, M. Waqas, S. Z. Abbas, M. Irfan, and T. Muhammad, J. Mater. Res. Technol. **15**, 306 (2021).
[46] H. Waqas, U. Farooq, M. Alghamdi, and T. Muhammad, Alex. Eng. J. **61**, 3949 (2022).
[47] S.-ur-Rehman, N. A. Mir, M. Farooq, M. Rizwan, F. Ahmad, S. Ahmad, and B. Ahmad, J. Mater. Res. Technol. **9**, 1631 (2020).